Al-Qadisiyah JournalFor Engineering Sciences 18 (2025) 403 – 415

Contents lists available at: http://qu.edu.iq

Al-Qadisiyah Journal for Engineering Sciences

Journal homepage: https://qjes.qu.edu.iq

Research Paper

An innovative graph-based approach for the topological structure of planetary gear mechanisms

Nabeel Almuramady [1]✉, ***M. F Al-Mayali*** [1], ***Essam L. Esmail*** [1], ***Mohammed A. Shallal Zahraa Aqeel A. Jassim*** [2], ***and Alaa F. Obaid*** [3]

[1]*Department of Mechanical Engineering, College of Engineering, University of Al-Qadisiyah Al-Diwaniyah, Iraq.*
[2]*Scientific Affairs, University of Al-Qadisiyah, Al-Diwaniyah, Iraq.*
[3]*Department of Chemical Engineering, College of Engineering, University of Al-Muthanna, Samawah, Iraq.*

ARTICLE INFO

Article history:
Received 07 November 2023
Received in revised form 12 May 2025
Accepted 24 September 2025

keyword:
Graph theory
Isomorphism
Planetary gear
Structure synthesis
Transmission

ABSTRACT

Planetary gear mechanisms (PGMs) are commonly employed in mechanical applications. Graph theory is a useful tool for synthesizing PGM structures to develop new transmission systems. The synthesis of 1 and 2 Degree-of-freedom (DOF) planetary gear trains received a lot of attention. Nevertheless, the synthesis results are inconsistent because previous graph representations were insufficient for the synthesis processes. This paper proposes a graph model that improves upon earlier models, introducing the concept of type-2 pseudo-isomorphic graphs. The vertex levels are used to construct PGM-spanning trees and define geared graphs. This approach avoids pseudo-isomorphic graphs and maintains a one-to-one correspondence between PGM elements and the graph. The 6-link 2-DOF PGM synthesis demonstrated the current graph representation, yielding 24 non-isomorphic mechanisms—11 more than previously reported. Possible explanations for the inconsistency of synthesis results with earlier studies are investigated, and the advantages of the modified graph over existing approaches are discussed.

1. Introduction

1.1 Graph representation and structural synthesis

Graph theory is the mathematical study of graphs used to build pairwise relationships between objects, and has gained importance in various fields such as operational research, chemistry, sociology, and genetics [1–7]. This is crucial in real-world applications, such as mechanical engineering design [8–10], where mechanisms within the same category, like planetary gear trains (PGTs), vary significantly. Mechanical engineering applications widely use PGTs due to their lightweight, high-speed reduction ratio, compact size, and differential drivability [11–14]. A planetary gear train (PGT) is a form of gear train in which some of the gears rotate around one or more central gears in addition to spinning around their own joint axis. Shafts mounted on a common stationary frame fit the central gears. The PGT represented in Fig. 1a is a one-degree-of-freedom PGT with two carriers and is composed of links 1, 2, 3, 4, 5, and 6. Bearings housed inside the frame (ground link 0) hold up the PGT, resulting in a two-degrees-of-freedom (DOF) fractionation mechanism that allows the PGT to freely spin with respect to its frame [15]. The revolute joints of the co-axial links 1, 3, 4, and 6 rotate around the principal axis of the central shaft (axis a). Planet gear refers to the gear that is not adjacent to the ground link. A typical PGM consists of a PGT supported by the frame along its common axis. A conventional graph, shown in Fig. 1b, can represent the PGT shown in Fig. 1a, according to Buchsbaum and Freudenstein [16]. In this graph, vertices are links, thin edges are revolute joints, and thick edges are geared joints. Figure 1c shows its graph representation using Yang et al.'s [17] perimeter loop graph model. Buchsbaum and Freudenstein [16] pioneered the use of graphs to demonstrate the topology of PGTs. A graph is a mathematical structure with vertices connected by edges that represent pair relations between links.

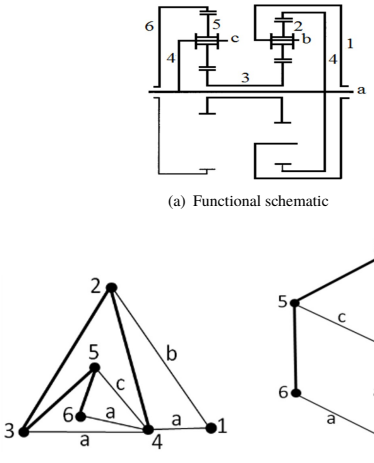

(a) Functional schematic

(b) Conventional graph

(c) Graph representation according to[17]

Figure 1. Simpson PGT and its graph representation.

*Corresponding Author.
E-mail address: Nabeel.almuramady@qu.edu.iq ; Tel: (+964) 782-114 5895 (Nabeel Almuramady)

https://doi.org/10.30772/qjes.2023.141737.1008

According to Buchsbaum and Freudenstein [16], the graph in Fig. 2a can represent the PGMs as shown in Fig. 2b, c, d, and e.

Nomenclature

d_i	The degree of a vertex i	m	The maximal degree of a vertex
DOF	Degree of Freedom	n	Number of Links
e	Number of edges	PGT	Planetary gear train
e_r	The number of revolute edges	PGM	Planetary gear mechanism
e_g	The number of geared edges	TV	Transfer vertex
F	Number of degrees of Freedom i	VDA	The vertex degree array
FC	Fundamental circuit	VDS	Vertex degree string
J	The total number of joints	V_k	The number of vertices of degree k (k=1,2,3,...,m)
J_r	The number of revolute joints	v	Number of vertices
J_g	The number of geared joints	V_m	Number of binaries, ternary...m-nary vertices
L	Number of independent loops i	$[V_m]$	Link assortment array for spanning tree
L_A	Link assortment		

Aside from the foregoing, Freudenstein [18] developed Boolean calculations to accurately predict the transfer vertex that corresponds to the planet carrier. Tsai and colleagues proposed "canonical graph representation"[19] to construct graphs that meet the structural properties of PGMs. Del Castillo and Salgado [20, 21] used a three-row graph to represent PGTs without idle links. One of the challenges in automating the parent graph technique [22] is determining the appropriate transfer vertex for each fundamental circuit. The procedure for drawing this kind of conclusion automatically is notably challenging [23]. Conventional graph representation makes a lot of pseudo-isomorphic graphs [24] when there are three or more coaxial links in a PGT. But when there are fewer than three coaxial links, it makes graphs with no specified principal axis [25]. These graphs lack a specified principal axis, allowing a single graph to represent multiple PGMs. PGM structure synthesis is a fast-expanding subject in mechanism investigations [26–37]. The primary goal of PGM structural synthesis was to generate a database that included all N-link and F-DOF-geared graphs. Shanmukhasundaram et al. [36] reviewed almost all of the algorithms used for PGT structure synthesis. All previous PGT synthesis methods excluded isomorphic graphs [38–46].

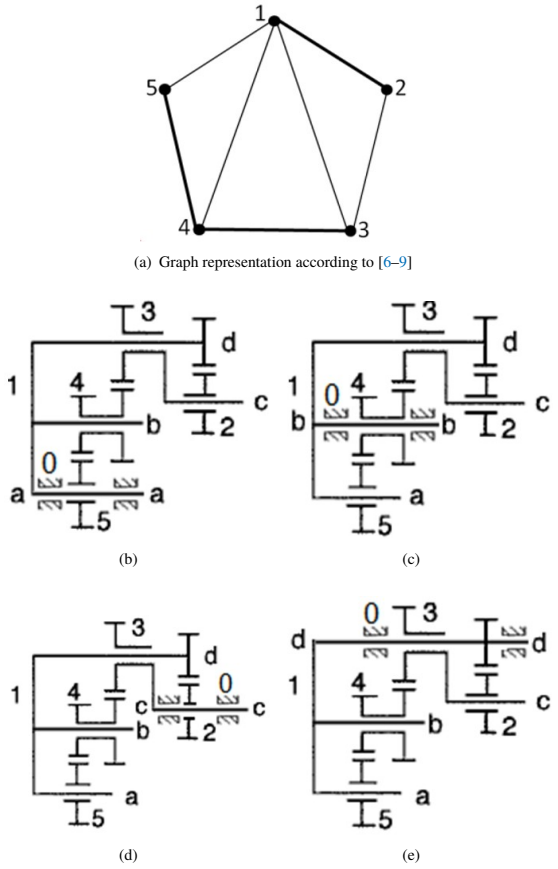

Figure 2. Graph and functional schematic representations with different principal axes.

Matching vertices, edges, and incidences makes two graphs isomorphic. The isomorphic test [**?**] uses the relationship between vertices and edges, which makes two graphs isomorphic. Hsu [37] and Tsai and Lin [47] synthesized the six- and seven-link two-DOF PGTs, whereas Yang et al. [23] synthesized PGTs with up to nine links. Abdali and Esmail [10] recently synthesized 7-link 3-DOF PGMs and discovered seven non-fractionated mechanisms—four more than before. Researchers have developed methods to enumerate PGTs, categorized into recursive, genetically compatible, parent-graph-based, and acyclic graph-based methods. According to previous research, the recursive technique does not enumerate the entire set of non-isomorphic graphs satisfying the given number of links and DOF [10, 28]. For a larger number of links, it is reasonable to assume that the recursive method will produce graph solutions that are far from complete (i.e., combinatorially). While the parent graph-based and acyclic graph-based methods are systematic and align with the structural synthesis of PGTs, they require the specification of a graph's principal axis to guarantee its uniqueness. Without specifying the principal axis, the graph lacks a hollow vertex or a solid polygon, resulting in a single graph representing multiple mechanisms. Furthermore, the inability of these graph models to generate multiple joints with fewer than three coaxial links prevents the generation of certain PGMs. Therefore, these graph models are unable to generate mechanisms with two coaxial links. One of the key motivations for using graph theory in mechanism design is that it allows for the investigation of all combinatorial possibilities. In this sense, the parent graph-based and acyclic graph-based methods are ineffective. Enumerating displacement graphs is a difficult combinatorial problem because it necessitates avoiding pseudo-isomorphic graphs, which are well described in the literature. Pseudo-isomorphic graphs are kinematically equivalent, mathematically non-isomorphic displacement graphs. As a result, the topological representation method for a displacement graph should be such that it is equal to all of its pseudo-isomorphs. In this context, the more recent displacement graph representation given by Yang et al. [17] is inappropriate since it produces a large number of type-2 pseudo-isomorphic graphs. A thorough review of the literature indicates the necessity for a systematic algorithm for constructing displacement graphs without producing pseudo-isomorphs.

1.2 Scope and contribution

Several graphs have been proposed in the literature to represent the structure of PGTs. Because most existing graph representation methods do not have one-to-one correspondences with PGTs, producing and representing graphs for all PGTs is inefficient in the following ways:

1. Two types of displacement graphs are used to represent PGTs: either with or without hollow vertices (solid polygons).
2. When the principal axis of a graph isn't specified, i.e., the graph contains no hollow vertex or solid polygon, a single graph represents several mechanisms.
3. Type-2 pseudo-isomorphic graphs, a concept introduced in this work, are unavoidable in the previous graph representations, and
4. Other models cannot create some PGMs. Multiple joints with fewer than three coaxial links cannot be produced via parent graph-based and acyclic-based methods.

This paper aims to analyze the shortcomings of previous graph representations of PGTs and to propose a modified rooted graph that allows for graph consistency, which will aid in the development of efficient and reliable structure synthesis tools. As a result, there is a need for an efficient and trustworthy graph representation for PGM synthesis, as well as an evaluation of existing kinematic synthesis results to validate the proposed rooted graph-based technique.

This is the first objective of this paper. This work describes the shortcomings of the graph representation of PGTs and proposes a modified rooted graph that ensures graph consistency. Graph theory knowledge is useful in building efficient algorithms for enumerating candidate graphs. The findings obtained with different methods for enumerating PGTs are frequently inconsistent due to the differences in the methods themselves. As a result, an effective and dependable structural synthesis method is required, as well as an evaluation of current results to validate the associated methodology. This is taken up as Objective 2, and the structural synthesis results of 6-link 2-DOF PGMs composed of PGTs with specified principal axes are utilized to determine the root causes of inconsistencies in previous synthesis results. The new model for planetary gear mechanisms is improved over prior ones due to its one-to-one representation with PGT, a single graph for a single mechanism, and the absence of Type-2 pseudo-isomorphic graphs. This study also addresses the limitations of other graph representations, including being unable to generate certain PGMs and the failure to construct multiple joints with fewer than three coaxial links.

1.3 Paper structure

We organize the paper as follows: Section 1 provides a summary of the key introductory principles, such as the rooted graph representation, pseudo-isomorphic mechanisms, vertex levels, and an introduction to graph representation. Section 2 discusses the creation of a modified graph representation that combines Hsu and Lam's graph representation and Tsai and colleagues' canonical graph representation. We introduce the concept of a "gray region,"defined as a subgraph consisting of all revolute edges with an identical label. As a result, identifying the edge levels is unnecessary because their features are already present in the rooted graph. Section 2 also introduces the concept of type-2 pseudo-isomorphic PGMs. Section 3 utilizes vertex levels, transfer vertices, and link assortments to create labeled spanning trees (rooted acyclic graphs). We build potential geared graphs from labeled spanning trees by designating transfer vertices and distributing geared edges. The newly proposed method solves the transfer vertex identification problems that are typical when automating any method. There are specific rules for incorporating geared edges with spanning trees and constructing geared graphs. Vertex-degree arrays are created and used to verify geared graphs. No graph can be considered a PGM if it violates the VDAs of the parent graph. Section 4 discusses the synthesis results of 6-link 2-DOF PGMs and serves as a summary of the work. Possible explanations for the inconsistent synthesis results with previous studies are explored. Finally, in section 5, certain conclusions are formed.

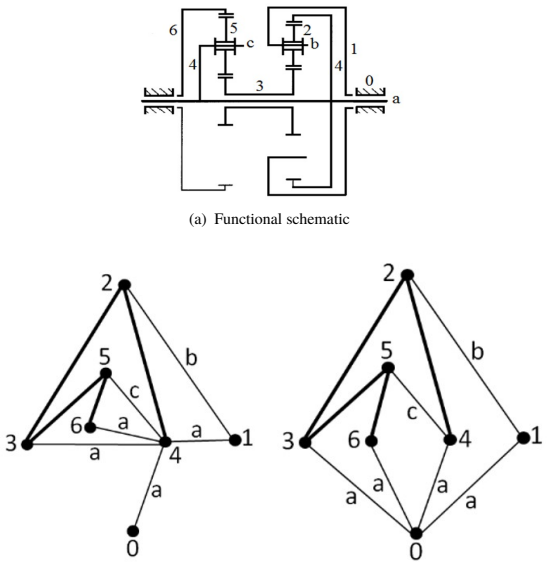

(a) Functional schematic

(b) Conventional graph representation

(c) Rooted graph representation

Figure 3**.** Simpson PGM and its rooted graph representation [15].

1.4 Basic introductory concepts

1.4.1 Rooted graph representation

The existing graph representation methods for the displacement graphs of PGTs need rotation graphs as the intermediate step. This paper proposes a method for directly obtaining displacement graphs, referred to here as rooted graphs, from functional schematic graphs. The rooted graph of a PGM is obtained as follows:

1. Create a conventional graph.
2. Delete all same-level revolute edges (excluding the one linked to the root), and
3. Connect the root vertex to the vertices that intersect at those same-level edges.

The first graph in Fig. 3 shows a conventional graph representation of both the PGT and the casing. Figure 3b illustrates the process of obtaining a rooted graph from Fig. 1a by removing the edges with label (a). Vertices 1, 3, and 6 are then joined to the root vertex designated "0". The PGT may have several movable carriers throughout space. This study will concentrate on PGMs, which are made up of PGTs held together by a fixed link (the casing).
The present work describes the shortcomings of graph representation and proposes a new graph that allows for graph consistency. The main objective of this paper is to suggest a modified graphic model of the PGM structure. The new graph representation is capable of completely avoiding the creation of pseudo-isomorphic graphs. In addition, it does not generate a single graph for PGMs with different principal axes. The paper outlines a technique for creating 2-DOF PGMs without isomorphic structures. Six-link 2-DOF PGMs are synthesized. Two graphs are considered isomorphic if their identification numbers match and they share the same spanning tree. Abdali and Esmail [50] present a procedure for finding and eliminating isomorphic graphs during the synthesis process of PGMs. In the present study, their method was used to detect isomorphism. To avoid redundancy and due to space limitations, the reader can return to the procedure details in the previous study. The method developed by Esmail [48] is utilized to eliminate degenerate structures during the synthesis process.

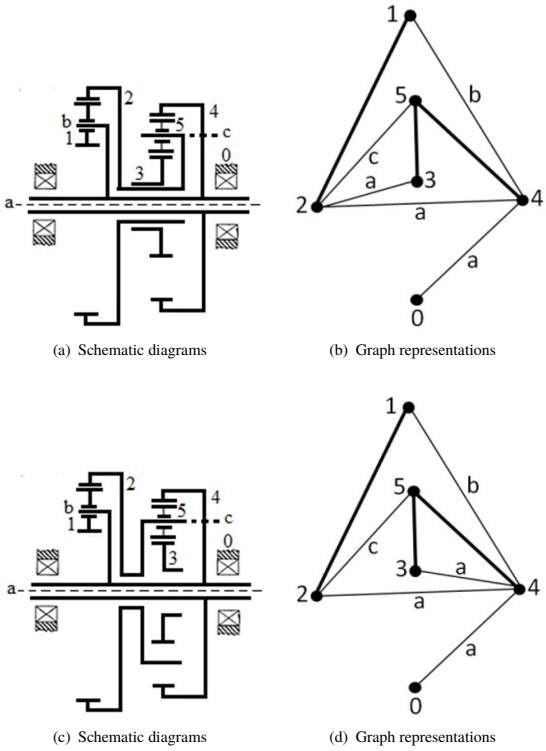

(a) Schematic diagrams

(b) Graph representations

(c) Schematic diagrams

(d) Graph representations

Figure 4**.** Planetary gear mechanisms.

1.4.2 Pseudo isomorphic mechanisms

It is difficult to represent a mechanism in a unique way on a graph because the graph can only represent binary joints. This is because a trinary joint can be represented by two binary joints made up of links 2 and 3, and 3 and 4, or by links 2 and 4, and 4 and 3. However, as a result, many revolute joints must share a common axis (they must be at the same level). A PGM composed of two or more coaxial links along a shared axis that are held up by the frame may comprise several pseudo-isomorphic mechanisms. As an illustration, rearranging the revolute joints between the coaxial links can transform the mechanism shown in Fig. 4a into the mechanism illustrated in Fig. 4c. Figures 4b and Fig. 4d show graphical representations of the two mechanisms. Although the two mechanisms are kinematically equivalent, the graphs are not mathematically isomorphic. Figure 4d is constructed by substituting the revolute edge

joining vertices 3 and 2 in the latter with a revolute edge of the same label connecting vertices 3 and 4 in the former. Figure 5 depicts the method for obtaining the rooted graph from Fig. 4b. The rooted graph in Fig. 5 can be constructed using Fig. 4d. The problem of pseudo-isomorphism is removed by using a rooted graph. In this paper, we shall refer to this kind of isomorphism as a type-1 pseudo-isomorphism.

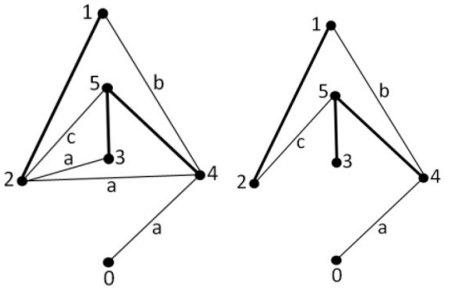

(a) Conventional graph

(b) All same-level revolute edges are deleted

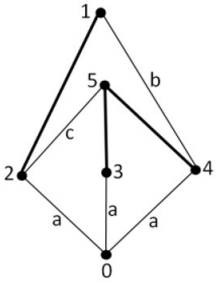

(c) Connect the same-level edges to the root vertex

Figure 5. Obtaining the rooted graph from Fig. 4b.

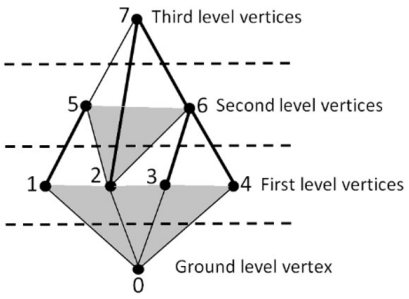

Figure 6. Vertex levels.

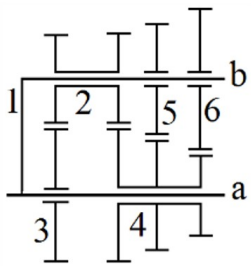

Figure 7. A PGT with a multiple-joint at the joint axis (a).

1.4.3 Vertex levels

Levels are assigned to vertices. The ground-level vertex represents the root. First-level vertices are located one revolution edge from the root; second-level vertices are two; and so forth. Figure 6 shows the vertex levels. A spanning tree contains details about all the revolute joints, their corresponding TVs, and their axes levels. The axes are required to draw a PGM out of a particular displacement graph. This discussion will be limited to the perimeter loop graph model because what applies to it also applies to other models.

1.5 An Introductory discussion of graph representation

1.5.1 Representation of PGTs by two types of graphs

A careful examination of the displacement graphs shown in Fig. 1c and Fig. 2a reveals two types of displacement graphs: Fig. 1c shows a graph with a hollow vertex (multiple joint or solid polygon), and Fig. 2a shows a graph without a hollow vertex or solid polygon. Even though Hsu and Lam [49, 50] presented graphs that could distinguish between multiple and simple revolute joints and Yang et al. [17] presented graphs with solid and hollow vertices, the graph in Fig. 2a is the same as the conventional graph represented by Buchsbaum and Freudenstein [16], i.e., it lacks a hollow vertex. In Refs. [22, 23, 25, 51, 52], PGTs are also presented by two kinds of graphs: graphs having a minimum of one hollow vertex (solid polygon) and graphs without any hollow vertex (solid polygon). Methods based on parent graphs and acyclic graphs may generate graphs lacking solid polygons or hollow vertices. The hollow vertex does not appear in the graphs of PGTs with fewer than three coaxial links [17, 22, 23]. The reason behind this is that PGT graphs are represented using the following rule: ïf a loop is entirely formed of revolute edges, the revolute edges in the loop are deleted, and the solid vertices in the loop are connected to a common hollow vertex by new revolute edges.Ä hollow vertex cannot exist if there are fewer than three revolute edges, so a loop cannot be formed. The multiple-joint or hollow vertex represents the revolute joints of coaxial links in PGMs, which revolve around the principal axis. Therefore, the principal axis is not stated in graphs that do not have a hollow vertex.

1.5.2 One graph represents several PGMs

When the principal axis of a graph isn't specified, i.e., the graph contains no hollow vertex, a single graph represents several mechanisms. For example, the difference between Fig. 2b and Fig. 2c is noticeable; gear 5 in Fig. 2b is a sun gear, whereas it is a planet gear in Fig. 2c. Although they represent two different mechanisms, they are represented by a single graph, as illustrated in Fig. 2a.

1.5.3 PGTs without graph representation

Figure 7 depicts a PGT with a multiple-joint at the joint axis (a). The revolute pairs of links 1, 3, and 4 all have an identical level (a) and correspond to a multiple joint of degree three. The perimeter-loop method [17] was not effective in identifying the graph for the PGT illustrated in Fig. 7 with a multiple-joint at the joint axis (a).

2. New modified rooted graph

The combination of Hsu and Lam's graph representation with Tsai and colleagues' canonical graph representation resulted in the development of a modified graph representation. The modified graph model has the following features:

1. All graphs feature at least one binary or multiple-joint called the root vertex, representing the revolute joints about the fixed link or housing of the mechanism.
2. The subset of a graph consisting of only the revolute edges with the same label that are connected to a shared lower-level vertex is commonly known as a "gray region."Modified spanning trees have as many labels as single edges and/or edge families (gray regions). The use of gray regions in spanning trees has the advantage of not requiring each edge to be labeled. All exhaustive labeling alternatives for the edges of a spanning tree can be replaced by spanning trees with gray regions.
3. For the first time, the concept of type-2 pseudo-isomorphic graphs is introduced in the graph representation of PGMs. When many gears in a PGM share a similar carrier on different joint axes and there is no geared joint between them, type-2 pseudo-isomorphic mechanisms are generated. For the graph representation presented by [17, 49, 52], type-2 pseudo-isomorphic graphs are unavoidable. The new graph model with gray regions eliminates the problem of type-2 pseudo-isomorphism at the outset.
4. The constituents of a rooted graph correspond one-to-one to those of a PGM. Table 1 shows this correspondence, while Table 2 includes some corresponding characteristics of PGMs and rooted graphs.

Table 1. Rooted graph corresponds with PGMs.

PGMs	S.	Rooted Graphs	S.	Correspondence relationship
Joints	J	Edges	e	$J = e$
Links	n	Vertices	v	$n = v$
Geared joints	J_g	Geared edges	e_g	$J_g = e_g$
Revolute joints	J_r	Revolute edges	e_r	$J_r = e_r$
Links having i joints	n_i	Vertices of degree i	v_i	$n_i = v_i$
Joints on link i	j_i	Degree of vertex i	d_i	$j_i = d_i$
Total loops	L	Total loops	L	$L = (L+1)$
Independent loops	$\overline{L}$	Ind. fundamental circuits	$\overline{L}$	$\overline{L} = n-1-F$

Table 2. Structural Characteristics of PGMs and Rooted Graphs.

Rooted Graphs	PGMs
$e = e_g + e_r$	$J = J_g + J_r$
$DoF = 3(v-1) - 2e_r - e_g$	$DoF = 3(n-1) - 2J_r - J_g$
$L = e - v + 1$	$L = J - n + 1$
$\sum_i d_i = 2\,e$	$\sum_i j_i = 2\,J$
$\sum_i v_i = v$	$\sum_i n_i = n$
$\sum_i i\,v_i = 2\,e$	$\sum_i i n_i = 2J$
$\sum_i i\,L_i = \overline{L} = L+1$	$\sum_i i\,L_i = \overline{L} = L+1$
Isomorphic rooted graphs	Isomorphic mechanisms

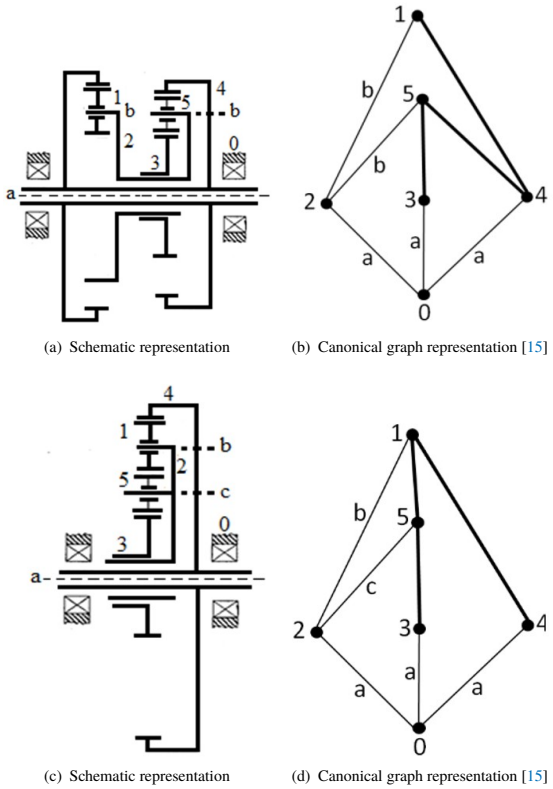

(a) Schematic representation (b) Canonical graph representation [15]

(c) Schematic representation (d) Canonical graph representation [15]

Figure 8. Planetary Gear Mechanisms.

2.1 Spanning trees

A tree is a connected graph that has (v-1) edges but no circuits. A single path connects any two vertices of a tree. By connecting any pair of non-adjacent vertices of a tree by an edge, a single circuit is created. Figure 8 shows the canonical graph representation of two PGMs. The modified spanning trees for the canonical representation of the graphs in Figs. 5 and 8 are illustrated in Fig. 9. All revolute edges of an identical label that are incident on a shared lower-level vertex form a family. Revolute edges of varied labels join vertices of distinct families to lower-level vertices. This results in a spanning tree with component subgraphs made up of all edges with the same label. For this reason, the subgraph created by the revolute edges with identical labels is referred to as a gray region. The subgraph produced by edges 0-2, 0-3, and 0-4, with the same label, generates a gray region in Fig. 9; edges 2-1 and 2-5 form another gray region in Fig. 9b. For a geared edge to connect two vertices, its path must contain exactly two levels. Gear edges cannot be used to connect two vertices on the same gray region. A geared edge cannot exist between the two second-level vertices (1 and 5) in Fig. 9b, but it is inevitable in Fig. 9c. A specific gray region contains revolute edges with identical levels, while all other revolute edges have unique levels. Thus, it is unnecessary to identify the edge levels, as their details already exist in the rooted graph. Modified spanning trees have as many labels as single edges and/or edge families (gray regions). All exhaustive labeling alternatives for the edges of a spanning tree can be replaced by spanning trees with gray regions. The path between two vertices where a geared edge is incident must have two revolute edges, two gray zones, or one of each. Gear edges can't be used to connect two vertices that are in the same gray region. A spanning tree of a rooted graph reveals transfer vertices (TVs), which can be used to locate all vertex pairings required to add gear edges. A fundamental circuit transfer vertex is a spanning tree vertex that is connected to more than two revolute edges, two gray regions, or a combination of both. Vertices 2 and 4 are the two TVs in Fig. 9a, while vertex 2 is the only TV in Figs. 9b and Fig. 9c. Any FC must have a geared edge and two labeled revolute edges separated by a TV.

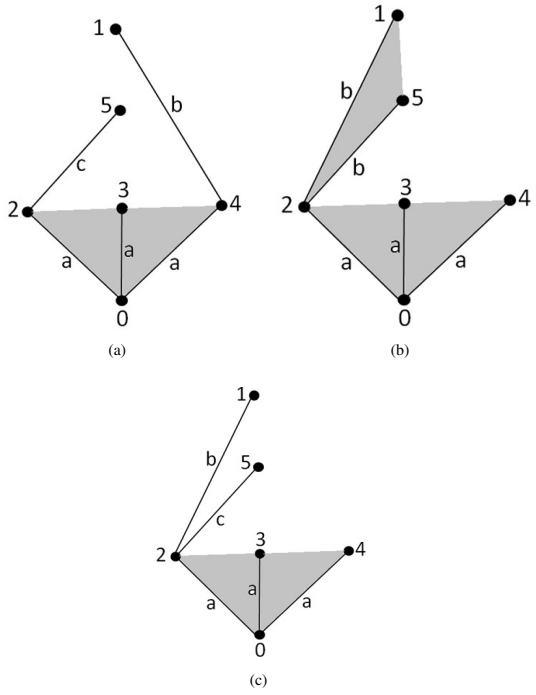

(a) (b) (c)

Figure 9. The modified spanning trees of Figs. 5 and Fig. 8.

2.2 Type-2 pseudo-isomorphic PGMs

Here, we introduce the concept of type-2 pseudo-isomorphic PGMs. When many gears in a PGM share a common carrier on different joint axes and there is no geared joint between them, it is feasible to reposition the axes of these gears without influencing the performance of the PGM. Figures 10a and 10b show two PGMs that only vary in the labeling of the edge levels of links 1 and 5. Figures 10a and 1b display two PGMs with variations in the edge level labeling of links 1 and 5. In Fig. 10a, links 1 and 5 are labeled on distinct joint axes "bänd "c", whereas in Fig. 10b, they are on the same joint axis "b". They are structurally non-isomorphic, but equivalent in terms of their functions, making them isomorphic. These kinematically equivalent PGMs are referred to as "type-2 pseudo-isomorphic"PGMs. If the levels of co-shaft links are considered identical, all possible type-2 pseudo-isomorphic mechanisms can be depicted using just one graph. The levels of links 1 and 5 in Fig. 10a can be moved to be at the same level as depicted in Fig. 10b, with no effect on the PGM's functionality. Therefore, the corresponding graphs of these two PGMs can be displayed as a single graph, as illustrated in Fig. 10c.

Table 3. Spanning trees for VDAs.

(4,2,1,1,1,1) ⇒	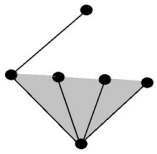	(3,3,1,1,1,1) ⇒	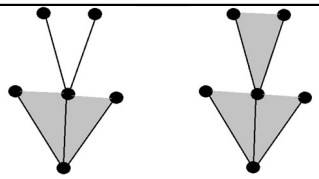
(3,2,2,1,1,1) ⇒	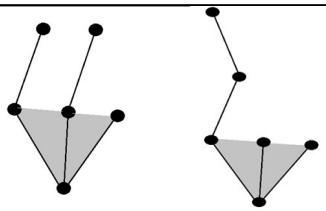	(2,4,1,1,1,1) ⇒	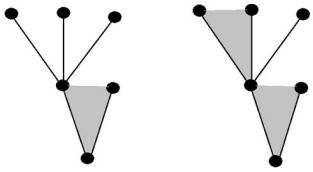
(2,4,1,1,1,1) ⇒	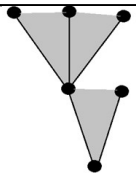	(2,3,2,1,1,1) ⇒	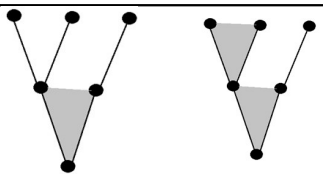
(2,3,2,1,1,1) ⇒	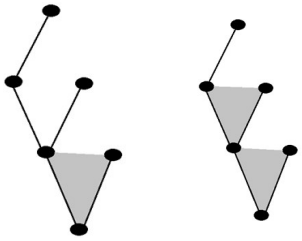	(2,2,3,1,1,1) ⇒	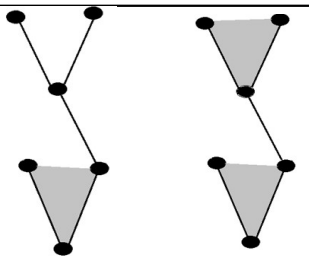
(2,2,2,2,1,1) ⇒	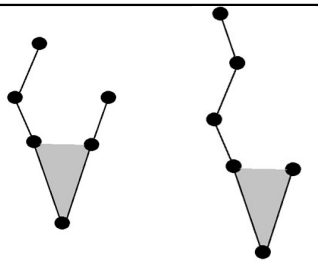		

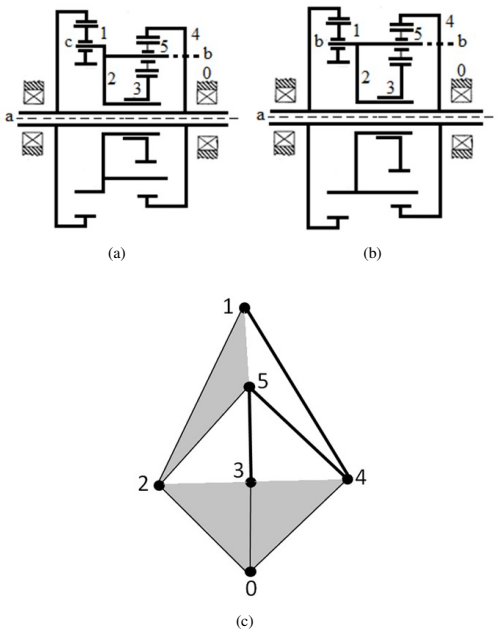

Figure 10. Type-2 pseudo-isomorphic PGMs.

3. Synthesis of PGMs

3.1 Generation of spanning trees and labelled graphs

The subsequent Eq. 1 and Eq. 2 can be utilized to construct spanning trees Eq. 1.

$$V_i + V_i + \ldots + V_m = v \tag{1}$$

Where v refers to the number of vertices, m refers to the maximal degree of a vertex, and V_k refers to the number of vertices of degree k ($k = 1, 2, 3, \ldots, m$), Eq. 2.

$$V_1 + 2V_2 + 3V_3 + \ldots + mV_m = 2(v-1) \tag{2}$$

For a 6-vertex spanning tree, Eq. 1 and Eq. 2 yield four-link assortments (LAs), namely [4, 1, 0, 1], [4, 0, 2, 0], [3, 2, 1, 0], and [2, 4, 0, 0]. Link assortments are used to generate the vertex degree arrays (VDAs). VDAs are utilized to draw the spanning trees. Classifying spanning trees into various categories is possible by examining the order of the gray region, which is numerically equivalent to the number of edges in the region with the same label.

Type 1: [4,2,1,1,1,1]
Type 2: [3,3,1,1,1,1], [3,2,2,1,1,1]
Type 3: [2,4,1,1,1,1], [2,3,2,1,1,1], [2,2,3,1,1,1], and [2,2,2,2,1,1].

The graphs that correspond to the above VDAs are displayed in Table 3. The TVs can be easily identified in a spanning tree using the newly developed method. A TV of fundamental circuits (FCs) is any vertex in a spanning tree

that is incident with a minimum of two single edges, two gray regions, or their combinations.

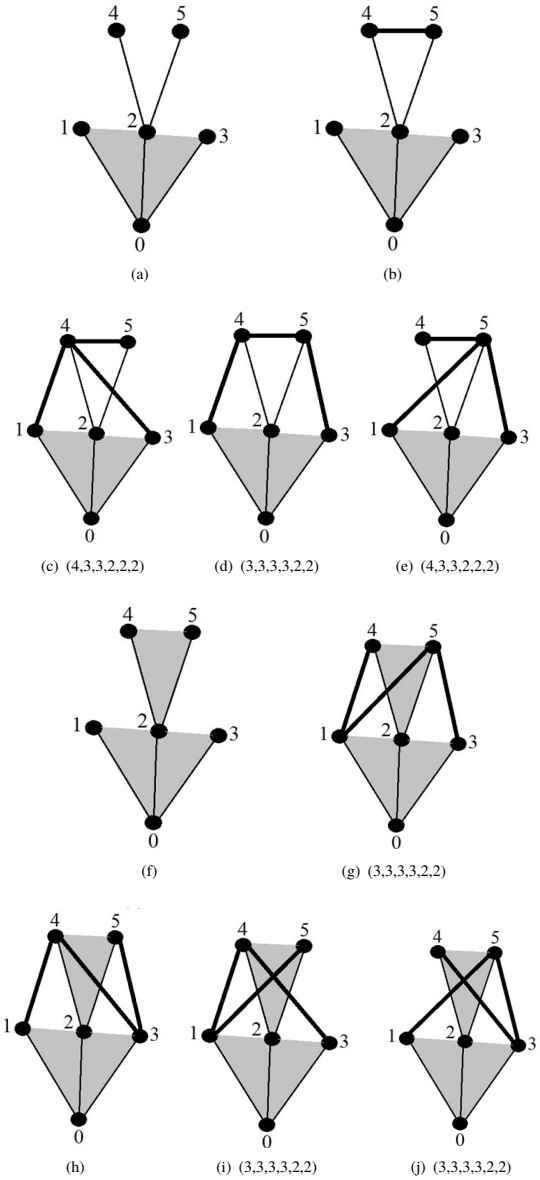

Figure 11**.** The addition of geared edges to spanning trees and the associated VDAs.

Because all labeled spanning trees do not have isomorphic tree topologies, displacement graphs from them should be created before doing an isomorphism check to generate a comprehensive variety of alternatives. Labeled spanning trees are utilized to identify transfer vertices and distribute geared edges, resulting in possible geared graphs. The gearing graphs are validated using the VDAs. Rather than fitting all spanning trees with parent graphs, geared graphs that do not conform to the VDAs of the parent graphs are eliminated. This improves the computational efficiency of the synthesis method.

3.2 Geared graph synthesis

Adding geared edges to spanning trees is frequently utilized to generate geared graphs. To connect two vertices, a geared edge must have two gray regions, two revolute edges, or one gray region and one revolute edge. An n-link 2-DOF PGM graph has n-3 geared edges and $L = e_g = n-1-F$ independent loops. Every possible link assortment for 6-link 2-DOF PGMs may be determined using the following two equations.

$$V_1 + V_3 + \ldots + V_m = v \tag{3}$$

$$2V_2 + 3V_3 + 4V_4 + \ldots + mV_m = 3e \tag{4}$$

with $v = 6$, $F = 2$, $e = 8$ and $m = 6-2 = 4$. Equations 5 and 6 were developed from Eqs. 3 and 4, respectively.

$$V_2 + V_3 + V_4 = 6 \tag{5}$$

$$2V_2 + 3V_3 + 4V_4 = 16 \tag{6}$$

Equations 5 and 6 can be solved to obtain three link assortments. Table 4 displays the link assortment (LA) and the VDAs of the geared graphs.

Table 4**.** Link assortments and VDAs.

LA	VDA
[2,4,0]	[3,3,3,3,2,2]
[3,2,1]	[4,3,3,2,2,2]
[4,0,2]	[4,4,2,2,2,2]

Geared graphs that fail to conform to the VDAs will be removed.

3.3 Adding geared edges

As an illustration of the concept of adding gearing edges, Figs. 11a and 11F depict the spanning trees for the VDA [3, 3, 1, 1, 1, 1]. A total of three geared edges is required. Since vertices 4 and 5 in Figs. 11a and 11f are connected to only one vertex, vertex 2; two different scenarios can occur. In the first scenario, illustrated in Fig. 11b, the graph can be completed by adding only two more geared edges. This is because one geared edge already connects the two vertices on the second level. To prevent creating a redundant link, connect the two two-level vertices (1 and 3) to the two second-level vertices. Given that the two geared edges may be shared by the two second-level vertices, three different configurations are feasible. There are three possible combinations: (2+0), (1+1), and (0+2). The graphs resulting from the (2+0) and (0+2) distributions are isomorphic due to the similarities between vertices 1 and 3, as depicted in Fig. 11c and 11e. These graphs will be further examined below. As shown in Figs. 11c and 11d, there are only two distinct, non-isomorphic ways to distribute the three geared edges among the two vertices at the first level. In the second scenario, the two vertices on the second level are not connected by a geared edge. Since vertex 2 on the first level is connected to the second level vertices 4 and 5, there are only two possible distributions in which the three geared edges connect those two vertices to vertices 1 and 3 on the first level. In terms of the arrangement of the geared edges between the vertices on the second level, two possible configurations exist. They can also be distributed in two distinct ways between the first-level vertices. Three isomorphic graphs result from the four distributions depicted in Figs. 10g, 10h, . 10i, and 10j. Thus, as shown in Fig. 11g, we have exactly one graph that is not isomorphic. It is crucial at this point to confirm the isomorphism of all graphs generated. Table 5 provides an exhaustive list of the results of graphs that are not isomorphic.

4. Results and discussion

4.1 Structural synthesis results

This paper presents our proposal for synthesizing 2-DOF PGMs, as well as the modified graph. A PGM typically consists of a PGT that the housing holds up along a common axis. With the housing supporting the PGT, the resulting PGM is a fractionation mechanism that gives the PGT an additional DOF to spin with respect to the housing freely. First, the present work describes the shortcomings of graph representation and proposes a modified graph that allows for graph consistency. When a PGT has three or more co-axial links, the conventional graph representation generates a large number of pseudo-isomorphic graphs, whereas when there are fewer than three co-axial links, graphs with no specified principal axis are generated. Because the principal axis in these graphs is not specified, a single graph represents several PGMs. The new graph representation is capable of completely avoiding the formation of type 1- and type 2-pseudo-isomorphic graphs, a concept that is first introduced in this work. In addition, it does not generate a single graph for PGMs with different principal axes. Second, the synthesis of 2-DOF PGM-spanning trees follows Eqs. 1 and 2. The improved approach using gray-region spanning trees is used to create all exhaustive labeling possibilities for the edges of non-isomorphic tree topologies. They are created using vertex levels, transfer vertices, and VDAs. A transfer vertex is a spanning tree vertex that connects two revolute edges, two gray regions, or both. Table 3 shows an extensive list of sixteen grey-region-spanning trees. Third, the labeled spanning tree atlas is used to create 2-DOF PGMs, generating potential graphs by detecting transfer vertices and distributing geared edges. The procedure involves generating three

vertex-degree arrays of geared graphs, as illustrated in Table 4, validating them, and comparing isomorphic identification numbers. The geared graphs that originate from various spanning trees do not have the same structure. Notably, geared graphs formed from different spanning tree types cannot be isomorphic. Section 3.3 outlines requirements for geared edges, while Table 5 displays the twenty-four non-isomorphic gearing graphs for 6-link 2-DOF PGMs.

4.2 Results comparison and validation

Unlike earlier findings by Hsu and Hsu [51], Yang and Ding [22], and Shanmukhasundaram et al. [52], twenty-four non-isomorphic mechanisms are revealed. The 6-link 2-DOF PGM synthesis results are summarized in Table 6.

Table 5. The synthesis results of generating geared graphs.

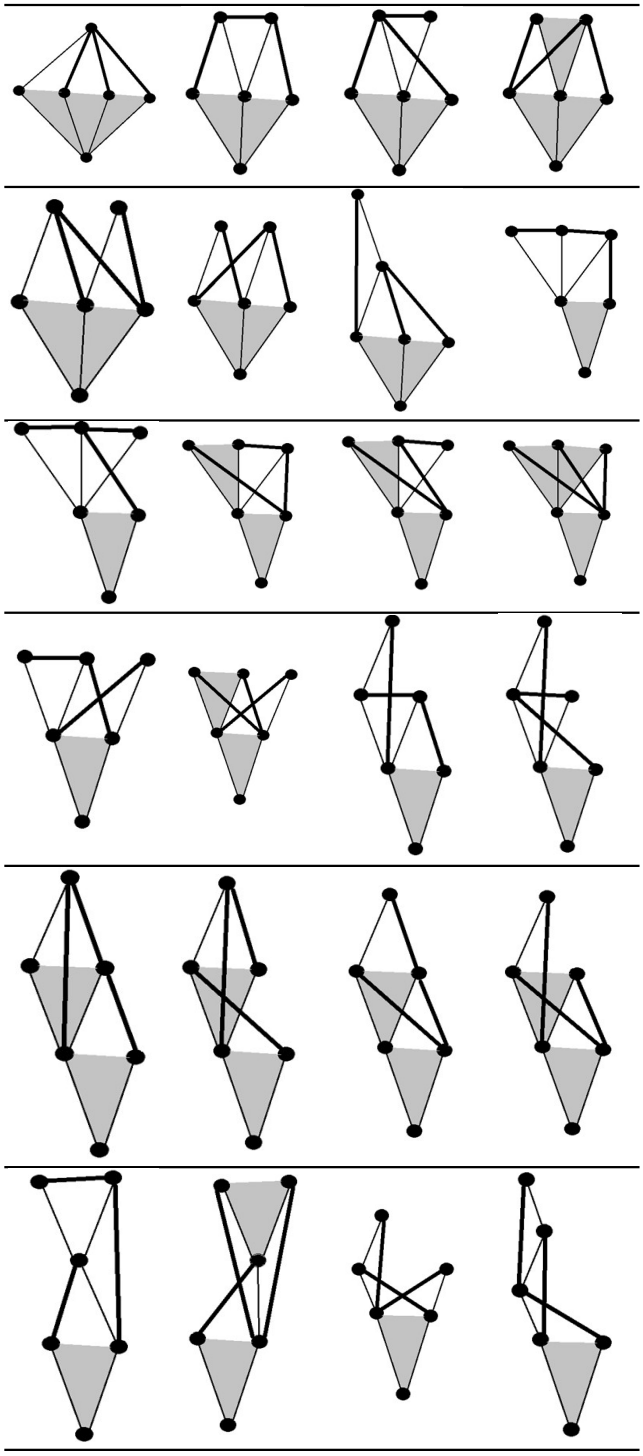

Yang and Ding [22] used the parent graph method to enumerate 13 displacement graphs for the 5-link 1-DOF PGTs. The 13 graphs are listed in the third column of Table 7. Upon closer inspection of the thirteen displacement graphs, two distinct kinds become apparent: those having multiple joints (hollow vertices) and those lacking such joints. A hollow vertex can be found in the graphs labeled "1-2", "1-3", "2-2", "2-3", "2-4", "3-2", "4-2", and "6-1". As a result, each of these eight graphs corresponds to a different 6-link 2-DOF PGM with the stated functional properties, with the exception of the graphs labeled "2-3änd "2-4", which correspond to a single graph. The hollow vertex corresponds to the common joint axis of the coaxial revolute joints that are connected to the casing. Because the hollow vertex corresponds to the root in the current graph representation, the graphs of the current method are completely identical to those of the Yang and Ding methods. The graphs with no hollow vertex labeled "1-1,2-1,3-1,4-1,änd "5-1äre PGTs, but their joint axes are not specified.

Table 6. Non-isomorphic geared graph synthesis.

$n-PGT$	$n-PGM$
5	6
No. of labelled trees	2-DOF PGMs
16	24

4.3 Causes of conflicting results

4.3.1 Kinematic inversions

One distinguishing aspect of PGMs is the presence of coaxial revolute joints, which attach certain PGT links to the casing. Connecting various PGM joint axes to the casing does not impact the relative motions of the links. Their motions with respect to the ground, however, might be distinct. Multiple PGMs can be created from a single PGT by selecting different common joint axes.

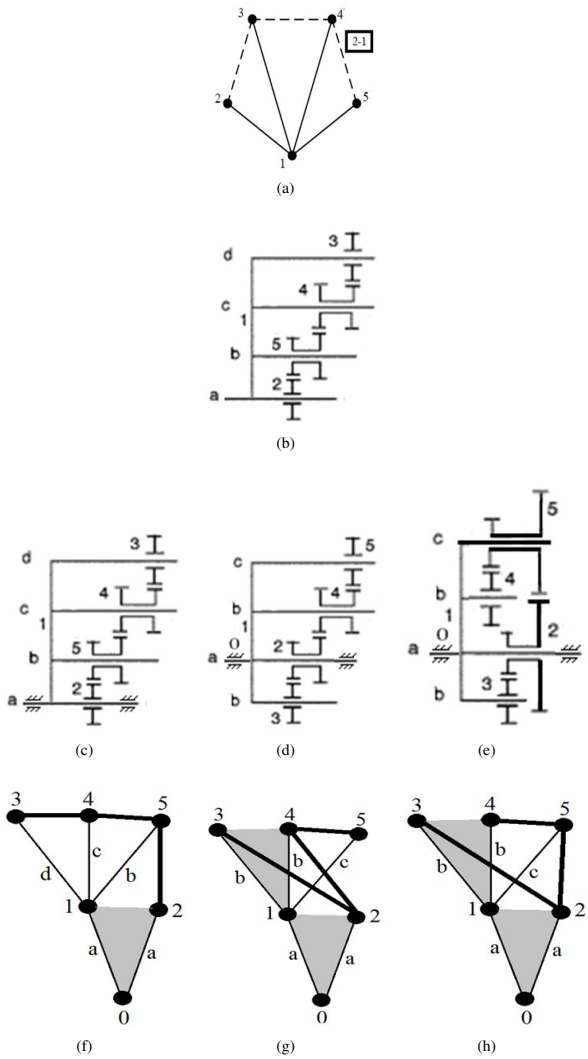

Figure 12. Three PGMs that all have the same PGT.

Table 7. Results comparison.

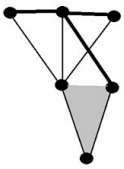	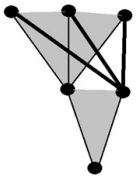	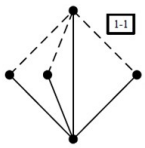	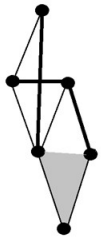	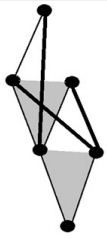	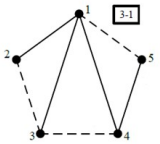
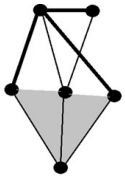	———	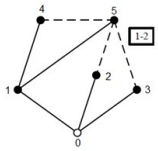	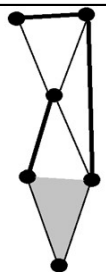	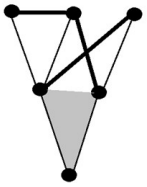	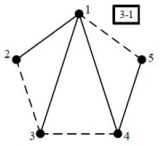
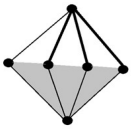	———	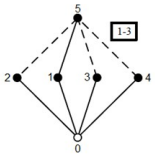	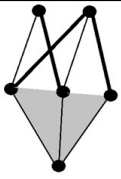	———	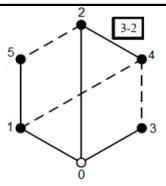
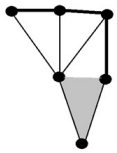	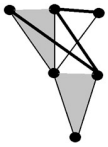	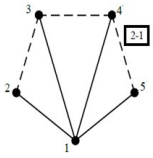	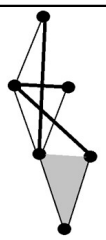	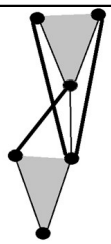	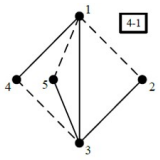
———	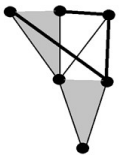	———	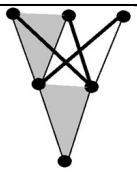	———	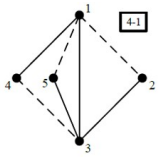
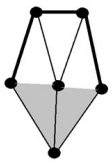	———	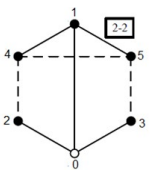	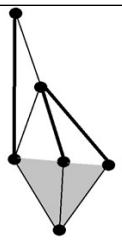	———	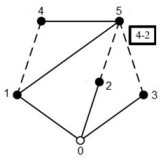
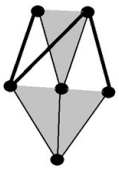	———	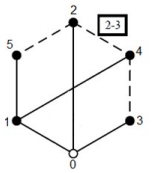	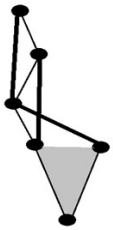	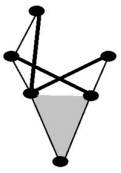	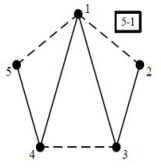
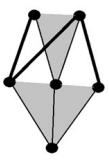	———	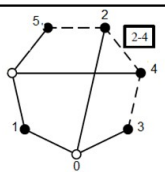	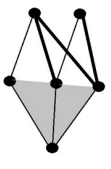	———	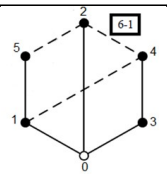

The hollow vertex or root distinguishes PGT from PGM. For example, the PGT depicted in Fig. 12b corresponds to the graph labeled ”2-1ín Fig. 12a. Examining the three PGMs dedicated to Figs. 12c, 12d, and 12e, where the common joint axes are labeled as ä”, we obtain their rooted graphs in Fig. 12f, 12g, and 12h. As a result, the number of graphs with no hollow vertex is less than the number of rooted graphs predicted by the new method.

4.3.2 PGMs with two coaxial links

Another possible explanation is that other models cannot create some PGMs. Multiple joints with fewer than three coaxial links cannot be produced via parent graph-based methods. This is related to the PGT graph representation method, which deletes revolute edges in a loop and joins solid vertices to a common hollow vertex. Parent graph-based approaches cannot produce degree-two hollow vertices due to the inability to construct a loop and the absence of a hollow vertex with less than three revolute edges. Therefore, mechanisms like the one shown in Fig. 13a cannot be created by it. Three new rooted graphs are shown in Fig. 13b.

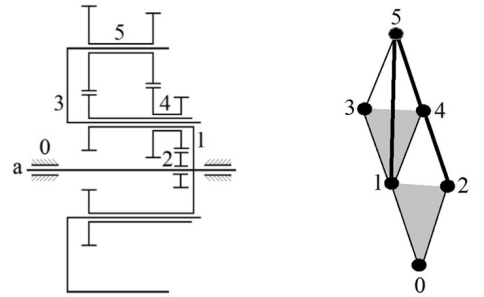

(a) Mechanism and its rooted graph

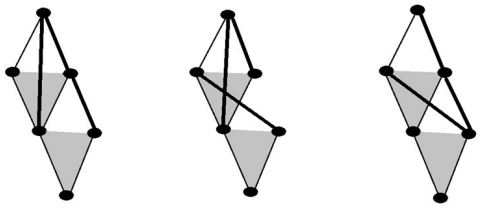

(b) Three novel rooted graphs

Figure 13**.** A new mechanism and its rooted graph.

4.3.3 Type-2 pseudo-isomorphic PGMs

The two types-2 pseudo-isomorphic PGMs illustrated in Figs. 10a and 10b are represented by two graphs using the perimeter loop method [17]. They are depicted in Figs. 14a and 14b. This graph model requires hollow vertices to represent groups of revolute edges with the same label in a graph. This addition increases the number of vertices and revolute edges. Figures 14a and 14b differ not just in edge labeling, but also in the number of vertices and edges. This creates a mismatch between the functional schematic and the perimeter-loop graph representations. Because of these differences, hollow vertices cannot be handled in the same way that solid vertices are.

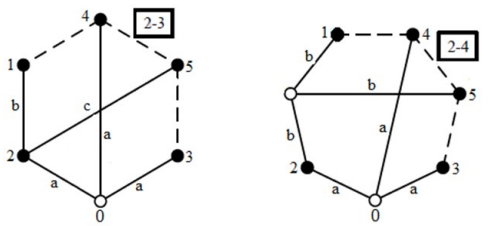

(a) The corresponding graph for the PGMs in Fig.10a according to [17].

(b) The corresponding graph for the PGMs in Fig.10b according to [17].

Figure 14**.** Two type-2 pseudo-isomorphic graphs.

4.3.4 Inappropriate graph representation

For a v-vertex graph, the degree of freedom (F) is calculated using the formula given in reference [10].

$$F = 3 \times (v-1) - 2 \times e_r - 1 \times e_g \tag{7}$$

where $e_g = v - 1 - F$ is for geared edges and $e_r = v - 1$ it is for revolutionary edges. We have $v = 7$, $e_r = 6$, and $e_g = 3$ for the graph in Fig. 14b. Equation 7 gives $F = 3(7-1) - 26 - 3 = 3$. Vertex selection refers to the process of removing one revolute edge and replacing it with one of the same level. Using this approach, the graph depicted in Fig. 15a can be transformed into Fig. 15d, which includes two separate vertices. This makes it a 3-DOF fractionated PGM. For the graph in Fig. 15d, v = 5, e_r= 4, and e_g= 3 that gives F = 1. Therefore, it is a 5-link 1-DOF PGT. The displacement graph in Fig. 14b does not correspond exactly to the PGT or PGM in Fig. 10b. Hence, the parent graph model is unable to appropriately represent a PGM with multiple joints. Due to difficulties with the parent graph model, the PGM graph, which includes multiple joints, was represented using a rooted graph model. Furthermore, all approaches based on parent graphs and acyclic graphs create graphs without multiple joints; however, this study finds that any graph includes at least one multiple joint, which is typically a root vertex. Therefore, the current rooted graph representation is more consistent than previous proposals.

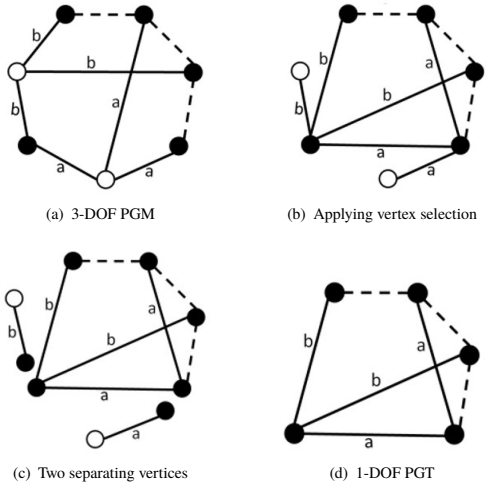

(a) 3-DOF PGM

(b) Applying vertex selection

(c) Two separating vertices

(d) 1-DOF PGT

Figure 15**.** Fractionation process for the graph seen in Fig. 14b.

4.4 PGTs versus PGMs

PGTs, as previously stated, are PGMs that lack a fixed link. For example, Fig. 16a shows a PGT with two joint axes. The significant difference between PGM and PGT arises from the presence of coaxial revolute joints that join specific links to the casing. The joint axis of the PGM determines these joints. Two inversions can be derived based on which joint axis is connected to the casing. They are shown in Figs. 16b and 16c. The resulting 7-link PGMs consist of one-DOF PGTs supported by the mechanism housing on the central axis. Figures 16d and 16e display the rooted graphs for the two non-isomorphic PGMs. Since the levels of the co-shaft links can be made identical, the PGM shown in Fig. 16f is considered to be type-2 pseudo isomorphic to the PGM shown in Fig. 16b, while the PGMs shown in Figs. 16g, 16h, and 16i are considered to be type-2 pseudo isomorphs of the PGM displayed in Fig. 16c. Therefore, Figs. 16d and 16e are the only two non-isomorphic graphs representing the two kinematic inversions of the PGT shown in Fig. 16a. In the perimeter-loop graph representation, the joint axis or multiple joints are represented by a hollow vertex [17]. It also generates the PGTs based on the biggest vertex degree string (VDS) [46] while excluding the smallest. Since the PGT shown in Fig. 16b has the largest VDS, the PGT shown in Fig. 16c is excluded because its VDS is smaller. Therefore, the perimeter-loop graph representation approach fails to capture the mechanism shown in Fig. 16c. The perimeter-loop graph representation of the two PGTs is shown in Figs. 16b and 16f are shown in Figs. 17a and 17b. The type-2 pseudo-isomorphic PGTs are represented by two non-isomorphic graphs. Additionally, the type-2 pseudo-isomorphic PGTs, illustrated in Figs. 16g, 16h, and 16i are represented by three non-isomorphic graphs in Figs. 18a, 18b, and 18c. Therefore, the perimeter-loop graph representation generates several type-2 pseudo-isomorphic PGTs.

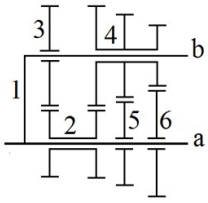

(a) A PGT with two joint axes.

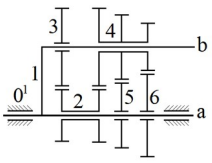

(b) A PGT with a joint axis at a.

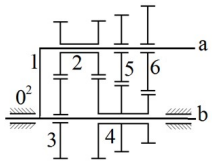

(c) A PGT with a joint axis at b.

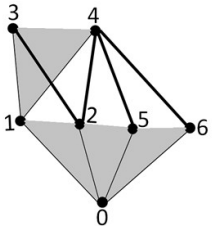

(d) Rooted graph for the PGT at (b)

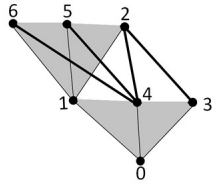

(e) Rooted graph for the PGT at (c)

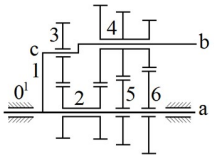

(f) Isomorphic to the PGM in Fig. 16 (b)

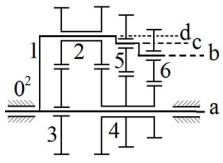

(g) Isomorphic to Fig. 16 (c)

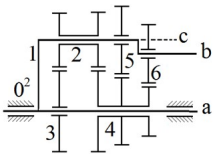

(h) Isomorphic to the PGM in Fig. 16 (c)

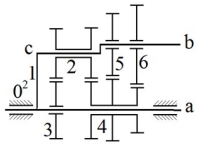

(i) Isomorphic to the PGM in Fig. 16 (c)

Figure 16**.** Kinematic inversions and their type-2 pseudo-isomorphic PGMs.

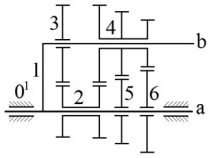

(a)

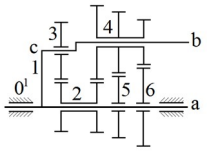

(b)

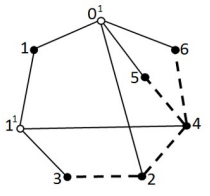

(c)

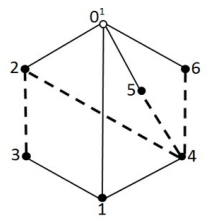

(d)

Figure 17**.** a and b are two type-2 pseudo-isomorphic PGTs represented by c and d, which are two non-isomorphic perimeter-loop graphs.

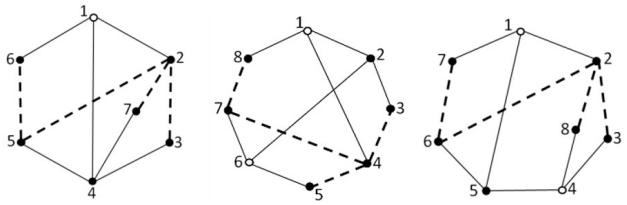

(a) (b) (c)

Figure 18**.** Three type-2 pseudo-isomorphic PGTs represented by three non-isomorphic perimeter-loop graphs.

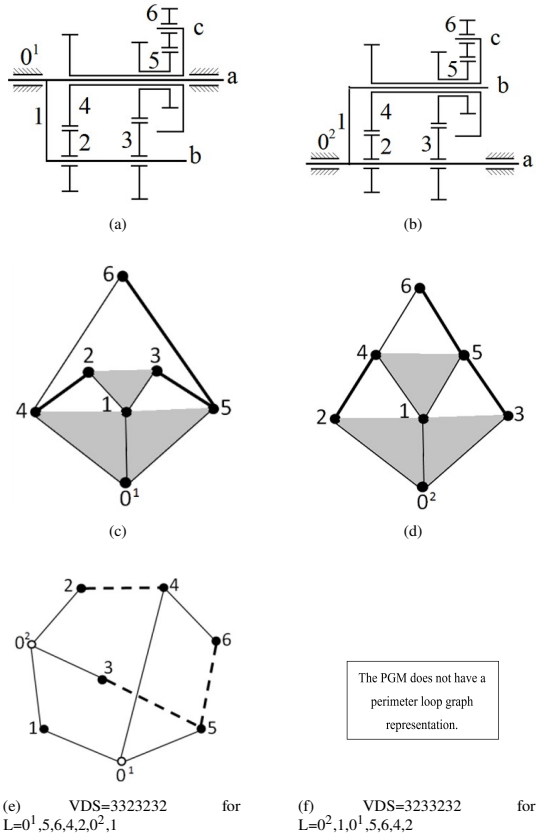

(a) (b) (c) (d)

(e) VDS=3323232 for L=0^1,5,6,4,2,0^2,1

(f) VDS=3233232 for L=0^2,1,0^1,5,6,4,2

Figure 19**.** The PGM with the largest vertex degree string has a graph representation.

4.5 PGMs without graph representation

The current rooted graph has a one-to-one correspondence to the PGM. When we examine the problem from a different point of view, we notice that although some PGTs have the same structure, their PGM structures differ. For example, Figs. 19a and 19b display feasible functional diagrams for the graphs in 19c and 19d of Fig. 19. Although the structures of both PGTs in 19a and 19b of Fig. 19 are the same, their PGM structures are not. In the perimeter loop graph technique, the PGM in Fig. 19a has a graph representation, whereas the PGM in Fig. 19b does not. The maximal degree string loop [46] forms the foundation of the perimeter loop method representation; this loop utilizes the largest VDS and disregards the others. In Fig. 19e, for instance, the degrees of the vertices 0^2, 1, 0^1, 5, 6, 4, and 2 are 3, 2, 3, 2, 3, and 2, respectively. Hence, the corresponding VDS is 3233232. In Fig. 19e, in the sequenced maximal loop L = 0, 1, 5, 6, 4, 2, 0, 2, 1, the degrees of the vertices 0^1, 5, 6, 4, 2, 0^2, and 1 are 3, 3, 2, 3, 2, and 2, respectively. As a result, the associated VDS is 3323232. The loop with the highest vertex degree string, 3323232, is the one with the maximum degree string. Consequently, the VDS 3233232 PGM is disregarded by the perimeter loop-based method. This is one of the reasons why many PGMs are often overlooked in perimeter loop-based techniques. The possibility that Fig. 19e represents the PGMs in Figs. 19a and 19b leads to the fact that the displacement graph and PGM do not have one-to-one correspondences.

5. Conclusions

This work addressed the challenge of modeling PGMs with multiple joints by using rooted graphs that correspond to the mechanism. It has been verified that the modified rooted graph has the following advantages:

- While parent graphs and acyclic graphs yield graphs without multiple joints, this study reveals that all graphs have at least one various joint, the root vertex.
- In a gray region, all revolute edges have the same level, whereas others have different levels. The rooted graph contains all edge information, eliminating the need for labeling.
- This graph model avoids pseudo-isomorphic graphs.
- It maintains a one-to-one correspondence between PGM elements and those of the rooted graph.
- Predicting PGMs with two co-axial links is more effective than acyclic graphs and parent graph-based methods due to constraints in their representation and technique.
- The current rooted graph model does not allow for a gear connection between two axes on the same shaft, which is a practical fact. Therefore, it avoids type-2 pseudo-isomorphic graphs, a concept that is first introduced in this work.
- The root vertex can be handled like any other vertex in the rooted graph model.

The study develops a new method for PGM synthesis that is an improvement over the existing approach. The vertex levels, link assortments, and transfer vertices are used to build labelled spanning trees. The synthesis of 6-link 2-DOF PGMs generated 24 non-isomorphic mechanisms, representing a considerable increase over previous studies. Possible explanations for the inconsistent synthesis results with previous studies are explored. Although the structure of some PGTs is the same, the structure of their PGMs is not. PGMs are identified by coaxial revolute joints, which connect PGT links to the housing. Connecting various joint axes does not affect the relative motions of the links; however, the ground motions may change. The significant difference between PGM and PGT arises from the presence of coaxial revolute joints that join specific links to the casing. All of the aforementioned modified graph advantages contribute to a simpler synthesis procedure and more reliable synthesis results. In the future, it is hoped that scholars will synthesize PGTs with more links and DOFs using the current graph model. However, inspection was used in the study to perform the structural synthesis. Because the synthesis procedure generates a huge number of graphs, an appropriate application could automatically create them. The automatic graph generation will make it easier to implement the synthesis results. It is also possible, using graph theory and symbolic notation, to generate unique identification codes for planetary gear mechanism structures. The obvious advantage is the production of a decodable atlas that can be stored in the computer's memory.

Authors' contribution

Nabeel Almuramady, *PhD*, and **M. F. Al-Mayali**, *PhD*, performed the analysis and wrote the first draft of the manuscript. **Essam L. Esmail**, *PhD*, modify the theoretical background and the concepts. **Mohammed A. Shallal**, *MSc*, reviewed and edited the manuscript. **Zahraa Aqeel A. Jassim**, *BSc* and **Alaa F. Obaid**, *MSc*, built the software program for analysis and presenting the result. All authors contributed to the ideation and investigations. All authors reviewed the manuscript before submission.

Declaration of competing interest

The authors declare no conflicts of interest.

Funding source

This study didn't receive any specific funds.

Data availability

The data that support the findings of this study are available from the corresponding author upon reasonable request.

REFERENCES

[1] A. Asghar, A. Qayyum, and N. Muhammad, "Different types of topological structures by graphs," *Eur. J. Math. Anal ysis*, vol. 3, no. 3, 2023. [Online]. Available: https://doi.org/10.28924/ada/ma.3.3

[2] A. El-Atik1, A. Nawar, and M. Atef, "Rough approximation models via graphs based on neighborhood systems," *Granular Computing*, vol. 6, p. 1025–1035, 2021. [Online]. Available: https://doi.org/10.1007/s41066-020-00245-z

[3] M. Atef, A. E. Atik, and A. Nawar, "Fuzzy topological structures via fuzzy graphs and their applications," *Soft Computing*, vol. 25, no. 4, pp. 1–15, 2021. [Online]. Available: https://doi.org/10.1007/s00500-021-05594-8

[4] J. Ma, M. Atef, S. Nada, and A. Nawar, "Certain types of covering-based multi granulation (i,t)-fuzzy rough sets with application to decision-making," *Complexity*, vol. 2020, no. 1, pp. 1–20, 2020. [Online]. Available: https://doi.org/10.1155/2020/6661782

[5] A. S. Nawar and A. A. E. Atik, "A model of a human heart via graph nano topological spaces," *international Journal of Biomathematics*, vol. 12, no. 01, p. 1950006, 2019. [Online]. Available: http://doi.org/10.1142/S1793524519500062

[6] N. Almuramady, M. F. Al-Mayali, and E. L. Esmail, "Configuration design and kinematic analysis of compound power-split mechanisms for in-wheel motor-driven electrical vehicles," *Results in Engineering*, vol. 28, p. 108368, 2025. [Online]. Available: https://doi.org/10.1016/j.rineng.2025.108368

[7] T. Ibraheem and A. A. Nagim, "On topological spaces generated by graphs and vice versa," *Journal of Al-Qadisiyah for computer science and mathematics*, vol. 13, no. 3, pp. 13–23, 2021. [Online]. Available: https://doi.org/10.29304/jqcm.2021.13.3.827

[8] Y. Lu and L. Xu., "Friction power loss of continuous sine tooth profile planetary reducer," *Results in Engineering*, vol. 20, p. 101640, 2023. [Online]. Available: https://doi.org/10.1016/j.rineng.2023.101640

[9] H. A. Hussen and E. L. Esmail, "Application of incidence matrix to topological structure and kinematic analysis of multi-planet gear trains," *Results in Engineering*, vol. 12, p. 100305, 2021. [Online]. Available: https://doi.org/10.1016/j.rineng.2021.100305

[10] H. A. Nafeh, E. L. Esmail, and S. H. Abdali, "Automatic structural synthesis of planetary geared mechanisms using graph theory," *Journal of Applied and Computational Mechanics*, vol. 9, no. 2, pp. 384–403, 2023. [Online]. Available: https://doi.org/10.22055/jacm.2022.41255.3721

[11] M. Li, L. Xie, and L. D. ., "Load sharing analysis and reliability prediction for planetary gear train of helicopter," *Mechanismand Machine Theory*, vol. 115, no. 1, p. 97–113, 2017. [Online]. Available: https://doi.org/10.1016/j.mechmachtheory.2017.05.001

[12] H. Ding, P. Huang, B. Zi, and A. Kecskeméthy, "Automatic synthesis of kinematic structures of mechanisms and robots especially for those with complex structures," *Appl. Math. Model*, vol. 36, no. 12, pp. 6122–6131, 2012. [Online]. Available: https://doi.org/10.1016/j.apm.2012.01.043

[13] T. Xie, J. Hu, Z. Peng, and C. Liu, "Synthesis of seven-speed planetary gear trains for heavy-duty commercial vehicle," *Mech. Mach. Theory*, vol. 90, no. 02, p. 230–239, 2015. [Online]. Available: https://doi.org/10.1016/j.mechmachtheory.2014.12.012

[14] M. Du and L. Yang, "A basis for the computer-aided design of the topological structure of planetary gear trains," *Mech. Mach. Theory*, vol. 145, p. 103690, 2020. [Online]. Available: https://doi.org/10.1016/j.mechmachtheory.2019.103690

[15] G. Chatterjee and L. Tsai, "Computer-aided sketching of epicyclic-type automatic transmission gear trains," *ASME J. Mech. Des.*, vol. 118, no. 3, p. 405–411, 1996. [Online]. Available: https://doi.org/10.1115/1.2826900

[16] F. Buchsbaum and F. Freudenstein, "Synthesis of kinematic structure of geared kinematic chains and other mechanisms," *J. Mechanisms*, vol. 5, no. 3, p. 357–392, 1970. [Online]. Available: https://doi.org/10.1016/0022-2569(70)90068-6

[17] W. Yang, H. Ding, B. Zi, and D. Zhang, "New graph representation for planetary gear trains," *ASME J. Mech. Des.*, vol. 140, no. 1, p. 012303(10 Pages), 2018. [Online]. Available: https://doi.org/10.1115/1.4038303

[18] F. Freudenstein, "An application of boolean algebra to the motion of epicyclic drives," *ASME J.Manufacturing and Engineering*, vol. 93, no. 1, p. 176–182, 1971. [Online]. Available: https://doi.org/10.1115/1.3427871

[19] L. Tsai, "The kinematics of spatial robotic bevel-gear trains," *IEEE Journal of Robotics and Automation*, vol. 4, no. 2, p. 150–156, 1988.

[20] J. D. Castillo, "Enumeration of 1-dof planetary gear train graphs based on functional constraints," *ASME J. Mech. Des.*, vol. 124, no. 4, p. 723–732, 2002. [Online]. Available: https://doi.org/10.1115/1.1514663

[21] D. R. Salgado and J. M. D. Castillo, "A method for detecting degenerate structures in planetary gear trains," *Mech. Mach. Theory*, vol. 40, no. 8, pp. 948–962, 2005. [Online]. Available: http://doi.org/10.1016/j.mechmachtheory.2004.12.019

[22] W. Yang and H. Ding, "The complete set of one-degree-of-freedom planetary gear trains with up to nine links," *ASME J. Mech. Des.*, vol. 141, no. 4, p. 043301, 2019. [Online]. Available: https://doi.org/10.1115/1.4041482

[23] W. Yang, H. Ding, and A. Kecskeméth, "Automatic structural synthesis of non-fractionated 2-dof planetary gear trains," *Mechanism and Machine Theory*, vol. 155, no. 1, p. 104125, 2021. [Online]. Available: https://doi.org/10.1016/j.mechmachtheory.2020.104125

[24] G. Chatterjee and L. Tsai, "Enumeration of epicyclic-type automatic transmission gear trains, sae," *Journal of Postcolonial Writing*, vol. 60, no. 2, p. 941012, 1994. [Online]. Available: http://doi.org/10.4271/941012

[25] V. Shanmukhasundaram, "Number synthesis and structure based rating of multilink epicyclic gear trains satisfying gruebler's degree of freedom equation. doctoral thesis, bits pilani – hyderabad campus, india," *International Journal of Science and Research Archive*, vol. 41, pp. 23–48, 2020.

[26] E. Pennestri and N. Belfiore, "On crossley's contribution to the development of graph based algorithms for the analysis of mechanisms and gear trains," *Mech. Mach. Theory*, vol. 89, no. 1, p. 92–106, 2015. [Online]. Available: https://doi.org/10.1016/j.mechmachtheory.2014.09.001

[27] L. Tsai, "An application of the linkage characteristic polynomial to the topological synthesis of epicyclic gear train," *ASME J. Mech., Transm. Autom. Des*, vol. 109, no. 3, p. 329–336, 1987. [Online]. Available: https://doi.org/10.1115/1.3258798

[28] J. Kim and B. Kwak, "Application of edge permutation group to structural synthesis of epicyclic gear trains," *Mech. Mach. Theory*, vol. 25, no. 5, p. 563–574, 1990. [Online]. Available: https://doi.org/10.1016/0094-114X(90)90070-Z

[29] J. Shin and S. Krishnamurthy, "Standard code technique in the enumeration of epicyclic gear trains," *Mech. Mach. Theory*, vol. 28, no. 3, p. 347–355, 1993. [Online]. Available: https://doi.org/10.1016/0094-114X(93)90075-7

[30] C. Hsu, K. Lam, and Y. Yin, "Automatic synthesis of displacement graphs for planetary gear trains," *Math. Comput. Model.*, vol. 19, no. 11, p. 67–81, 1994. [Online]. Available: https://doi.org/10.1016/0895-7177(94)90017-5

[31] Y. Rao and A. Rao, "Generation of epicyclic gear trains of one degree of freedom," *ASME J. Mech. Des.*, vol. 130, no. 5, p. 052604(8 pages), 2008. [Online]. Available: https://doi.org/10.1115/1.2890107

[32] R. Cui, Z. Ye, L. Sun, G. Zheng, and C. Wu, "Synthesis method for planetary gear trains without using rotation graphs," *Proceedings of the Institution of Mechanical Engineers, Part C:Journal of Mechanical Engineering Science*, vol. 236, no. 2, pp. 972–983, 2022. [Online]. Available: https://doi.org/10.1177/0954406221998399

[33] V. Kamesh, K. Rao, and A. Rao, "Topological synthesis of epicyclic gear trains using vertex incidence polynomial," *J. Mech. Des.*, vol. 139, no. 6, p. 062304, 2017. [Online]. Available: http://doi.org/10.1115/1.4036306

[34] S. V. R., R. Y. V. D., R. S. P., D.Varadaraju, and E.Pennestrì, "Structural synthesis and classification of epicyclic gear trains: an acyclic graph-based approach," *Advances in Industrial Machines and Mechanisms, 683, Lecture Notes in Mechanical Engineering, Springer, Singapore Periodicals of Engineering and Natural Sciences*, vol. 10, p. 683–707, 2021. [Online]. Available: https://link.springer.com/chapter/10.1007/978-981-16-1769-0_62#citeas

[35] E. L. Esmail and F. M. Saoud, "Creative design of planetary gear-cam mechanisms," *Results in Engineering*, vol. 19, no. 4, p. 101350, 2023. [Online]. Available: https://doi.org/10.1016/j.rineng.2023.101350

[36] V. Shanmukhasundaram, Y. Rao, and S. Regalla, "Review of structural synthesis algorithms for epicyclic gear trains. in: D. sen, s. mohan, g. ananthasuresh (eds)," *Mechanism and Machine Science. Lecture Notes in Mechanical Engineering. Springer, Singapore*, no. 8, p. 79–87, 2024. [Online]. Available: https://doi.org/10.1007/978-981-15-4477-4_25

[37] C. Hsu., "Synthesis of kinematic structure of planetary gear trains by admissible graph method," *J. Frankl. Inst.*, vol. 330, no. 5, p. 913–927, 1993. [Online]. Available: https://doi.org/10.1016/0016-0032(93)90085-9

[38] R. Rai and S. Punjabi, "A new algorithm of links labelling for the isomorphism detection of various kinematic chains using binary code," *Mech. Mach. Theory*, vol. 131, no. 8, p. 1–32, 2019. [Online]. Available: https://doi.org/10.1016/j.mechmachtheory.2018.09.010

[39] Y. H. J, W. J. P, H. Y. L, and Y. P, "Mechanism isomorphism identification based on artificial fish swarm algorithm," *Proceedings of the Institution of Mechanical Engineers, Part C: Journal of Mechanical Engineering Science*, vol. 235, no. 21, p. 5421–5433, 2021. [Online]. Available: https://doi.org/10.1177/0954406220977560

[40] Y. H. Zou and P. He, "An algorithm for identifying the isomorphism of planar multiple joint and gear train kinematic chains," *Mathematical Problems in Engineering*, vol. 2-16, no. 1, p. 5310582, 2016. [Online]. Available: https://doi.org/10.1155/2016/5310582

[41] H. T. T. P., H. F. D. Liu, and Y. Q. Zhao, "Isomorphism identification algorithm and database generation for planar 2–6 dofs fractionated kinematic chains combined by two or three non-fractionated kinematic chains," . *Mech. Mach. Theory*, vol. 166, no. 8, p. 104520, 2021. [Online]. Available: https://doi.org/10.1016/j.mechmachtheory.2021.104520

[42] L. Y., F. X. He, L. S. Liu, and W. C. Y., "Isomorphic identification for kinematic chains using variable high-order adjacency link values," *J. Mech. Sci. Technol.*, vol. 33, no. 10, p. 4899–4907, 2019. [Online]. Available: https://doi.org/10.1007/s12206-019-0930-9

[43] R. K. Rai and S.Punjabi, "Kinematic chains isomorphism identification using link connectivity number and entropy neglecting tolerance and clearance," *Mech. Mach. Theory*, vol. 123, no. 1, p. 40–65, 2018. [Online]. Available: https://doi.org/10.1016/j.mechmachtheory.2018.01.013

[44] K. V. V., K. M. Rao, and A. B. S. Rao, "An innovative approach to detect isomorphism in planar and geared kinematic chains using graph theory," *J. Mech. Des.*, vol. 139, no. 12, p. 122301(11pages), 2017. [Online]. Available: https://doi.org/10.1115/1.4037628

[45] C. H. Hsu, "Displacement isomorphism of planetary gear trains," *Mech. Mach. Theory*, vol. 29, no. 4, p. 513–523, 1994. [Online]. Available: https://doi.org/10.1016/0094-114X(94)90091-4

[46] W. Yang and H. Ding, "The perimeter loop-based method for the automatic isomorphism detection in planetary gear trains," *J. Mech. Des*, vol. 140, no. 12, p. 123302, 2018. [Online]. Available: https://doi.org/10.1115/1.4041572

[47] L. W. Tsai and C. C. Lin, "The creation of nonfractionated, two-degree-of-freedom epicyclic gear trains," *Journal of Mechanisms, Transmissions, and Automation in Design*, vol. 111, p. 524–529, 1989. [Online]. Available: https://doi.org/10.1115/1.3259033

[48] E. L. Esmail, "A matrix-based method for detection of degenerate structures in planetary gear trains," *Mechanism and Machine Theory*, vol. 175, p. 104925, 2022. [Online]. Available: https://doi.org/10.1016/j.mechmachtheory.2022.104925

[49] C. H. Hsu and K. T. Lam, "A new graph representation for the automatic kinematic analysis of planetary spur-gear trains," *ASME J.Mech.Des*, vol. 114, no. 1, p. 196–200, 1992. [Online]. Available: https://doi.org/10.1115/1.2916916

[50] C. H., Hsu, , and L. K. T., "Automatic analysis of kinematic structure of planetary gear trains," *ASME J. Mech. Des.*, vol. 115, no. 3, pp. 631–638, 1993. [Online]. Available: https://doi.org/10.1115/1.2919237

[51] C. Hsu and J. Hsu, "An efficient methodology for the structural synthesis of geared kinematic chains," *Mech. Mach. Theory*, vol. 32, no. 8, p. 957–973, 1997. [Online]. Available: https://doi.org/10.1016/S0094-114X(96)00081-X

[52] V. Shanmukhasundaram, Y. Rao, and S. Regalla, "Enumeration of displacement graphs of epicyclic gear train from a given rotation graph using concept of building of kinematic units," *Mech. Mach. Theory*, vol. 134, p. 393–424, 2019. [Online]. Available: https://doi.org/10.1016/j.mechmachtheory.2019.01.005

How to cite this article:
Nabeel Almuramady, M. F Al-Mayali, Essam L. Esmail, Mohammed A. Shallal, Zahraa Aqeel A. Jassim, and Alaa F. Obaid. (2025). 'An innovative graph-based approach for the topological structure of planetary gear mechanisms', Al-Qadisiyah Journal for Engineering Sciences, 18(4), pp. 403- 415.
https://doi.org/10.30772/qjes.2023.141737.1008